Study on Cathode Materials for Achieving IT-SOFC with Proton Conductor

M. Asamoto*, S. Miyake*, Y. Yonei*, H. Yamaura* and H. Yahiro *

* Department of Materials Science and Biotechnology, Graduate School of Science and Engineering, Ehime University, Matsuyama 790-8577, Japan, hyahiro@eng.ehime-u.ac.jp

ABSTRACT

The electrochemical performances of the perovskite-type oxide cathode with uniform particles were investigated in H_2-O_2 SOFC system using proton conductor. Among the perovskite-type oxides used in the present study, $La_{0.7}Sr_{0.3}FeO_3$ (LSF) exhibited the lowest cathodic overpotential at the temperature as low as 773 K. It was found that the overpotentials of LSF cathode and the activation energies of cathode reaction were influenced by the electrode morphologies such as particle size and uniformity. The electrophoretic deposition (EPD) as a new method was applied to fabricate the LSF cathode on electrolyte surface.

Keywords: cathode, proton conductor, fuel cell, perovskite-type oxide, EPD

1 INTRODUCTION

The doped perovskite-type oxide protonic conductors such as Yb-doped $SrCeO_3$ and Nd- or Gd-doped $BaCeO_3$ are of interest for their applications in hydrogen sensors [1], hydrogen pumps [2], membrane reactors [3], and fuel cells [4-7]. The use of proton-conducting electrolyte in solid oxide fuel cells (SOFCs) has some advantages compared with that of the oxide-ion conductor. For instance, the protonic ceramic fuel cells form water at the cathode compartment. It means that the fuel unreacted keeps pure at the anode compartment, requiring no recirculation.

The electrical conductivity of protonic ceramics was studied as a function of oxygen partial pressure [8]. In a hydrogen atmosphere corresponding to very reducing oxygen partial pressure, it is reported that the electrical properties of $SrCe_{0.95}Yb_{0.05}O_3$ (SCY) are dominated by the ionic conductivity at low temperature, while the electron conductivity becomes dominant at high temperature. For example, a transition from ionic to electronic conductivity in a hydrogen atmosphere was observed at about 1023 K for SCY [8]. This suggests that SOFC using SCY electrolyte should be operated below 1023 K. However, the decrease in the operating temperature results in an increase of the overpotential, mainly at the cathode. Therefore, the development of a superior cathode becomes an important subject to realize an intermediate temperature-solid oxide fuel cell (IT-SOFC) using protonic-conducting electrolyte.

Mixed conducting ABO_3 perovskite-type oxides in SOFC have received much attention as electrode materials. $La_{1-x}Sr_xMnO_3$ has been considered to be one of the most promising cathode materials for oxide ion-SOFCs [9]. As alternative candidates, $La_{1-x}Sr_xCoO_3$ [10], $La_{1-x}Sr_xFeO_3$ [11], and $La_{1-x}Sr_xMn_{1-y}Co(Fe)_yO_3$ [12] have been reported. However, little is known about the perovskite-type oxide cathode in SOFC using proton conductor.

Uchida et al. [13] reported about the mechanism of Pt cathode in SOFC using proton conductor. They suggested that the cathode reaction consists of the following five elementary steps and the surface diffusion of adsorbed oxygen atoms toward the electrochemically active sites on Pt (eq. (3)) is the rate-determining step.

$$O_2(g) \rightarrow O_2(ad) \quad (1)$$
$$O_2(ad) \rightarrow 2O(ad) \quad (2)$$
$$\text{surface diffusion of O(ad)} \quad (3)$$
$$O(ad) + 2H^+ + 2e \rightarrow H_2O(ad) \quad (4)$$
$$H_2O(ad) \rightarrow H_2O(g) \quad (5)$$

On the other hand, we reported that the either eq. (4) or (5) in above elementary steps is the rate-determining step for LSF cathode [14]. The cathode mechanism must be taken into consideration for the formation and diffusion of water, since water forms at the cathode in proton conductor fuel cell. In the present study, the perovskite-type oxides with uniform particles were utilized to investigate both the cathode performance and the cathode mechanism in H_2-O_2 fuel cell systems using SCY electrolyte. In addition, the electrophoretic deposition (EPD) method was applied to fabricate the perovskite-type oxide cathode on SCY electrolyte surface.

2 EXPERIMENTAL

2.1 Sample Preparation

Polycrystalline SCY electrolyte was prepared by conventional solid-state reactions [14]. The mixed powders, $SrCO_3$ (Wako, 95%), CeO_2 (Wako, 99.9%), and Yb_2O_3 (Wako, 99.9%), were calcined at 1673 K for 10 h in air. The resulting powders were ground and uniaxially pressed into pellets under a pressure of 2000 kg cm^{-2}. The obtained pellets were then sintered at 1773 K for 10 h in air. The diameter and the thickness of the sintered pellets were *ca.* 9 mm and *ca.* 2.3 mm, respectively. X-ray powder diffraction (RIGAKU RINT2000, CuK_α) pattern of SCY sample exhibited a single phase with the perovskite structure.

Cathode materials, $La_{0.7}Sr_{0.3}MO_3$ (M = Mn, Fe, and Co), were prepared by the solid-state reaction. La_2O_3 (Wako,

Clean Technology 2008, www.ct-si.org, ISBN 978-1-4200-8502-0

99.99%), $SrCO_3$ (Wako, 95%), $MnCO_3$ (Wako, 99%), Fe_2O_3 (Wako, 99.5%), and Co_3O_4 (Wako, >90%) were used as starting materials. These powders were mixed in appropriate ratio and ground in a ball mill with ethanol for 24 h. After drying, the mixed powders were calcined at 1673 K for 10 h in air. The resulting powders were ground by ball-milling for 10 and 30 h to obtain the fine particles.

Two methods, a conventional method and an EPD method, were utilized for fabricating cathode on the surface of electrolyte. A conventional method was performed as follows. $La_{0.7}Sr_{0.3}MO_3$ oxide powders was dispersed into turpentine oil (Wako, 90%) and painted on one face of electrolyte. After drying at room temperature for several hours, the sample was heat-treated at 1173 K for 3 h to obtain good adherence between cathode and electrolyte. An EPD method was performed according to the previous literature [15]. In this case, the sample was finally heat-treated at 973-1173 K.

2.2 Measurement of Cathodic Overpotentials

The construction of a H_2-O_2 fuel cell was essentially the same as that reported elsewhere [14]. The platinum was used as an anode. The electrolyte with electrodes was placed between silica tubes with glass gaskets to separate two compartments. A Pt wire was connected to a Pt-mesh current collector attached to each electrode. A Pt wire was wound around the side of the electrolyte as a reference electrode. Hydrogen gas saturated with water vapor at 298 K was supplied to the anode compartment at a flow rate of 50 $cm^3 \cdot min^{-1}$, while air as an oxidant gas was supplied to the cathode compartment at a flow rate of 50 $cm^3 \cdot min^{-1}$. A current interruption method using the reference electrode was employed to obtain cathodic overpotentials under the operation of a H_2-O_2 fuel cell at 773-973 K. The transient behavior of the electrode potential was measured by an oscilloscope (IWATSU SS-5510).

3 RESULTS AND DISCUSSION

3.1 Source Powders of $La_{0.7}Sr_{0.3}MO_3$

The XRD profiles of $La_{0.7}Sr_{0.3}MO_3$ samples with various B-site cations provided the single phase assigned to the perovskite-type structure; no diffraction peak from a secondary phase or from the starting materials was observed.

The particle size distributions of $La_{0.7}Sr_{0.3}FeO_3$ (LSF) powders ground by ball-milling for 10 and 30 h are given in Fig. 1, together with that of as-calcined LSF powder. It is obvious that the LSF powders ground by ball-milling are more uniform and finer than as-calcined LSF powder. The mean diameters of LSF powders ground by ball-milling for 10 and 30 h were estimated to be 1.8 and 0.8 μm, respectively. The resulting LSF powders were used to evaluate the cathodic performances in H_2-O_2 SOFC. Hereafter, the cathodes made from the LSF powders with the different distributions (I)-(III), as shown in Fig. 1, are represented by LSF (a)-(c), respectively.

$La_{0.7}Sr_{0.3}MnO_3$ (LSM) and $La_{0.7}Sr_{0.3}CoO_3$ (LSC) powders were also ground by ball-milling for 30 h. After ball-milling, the mean diameter of LSM and LSC particles was 0.4 and 0.5 μm, respectively, and the particle size distributions of LSM and LSC were very similar to that of LSF (Fig. 1(III)).

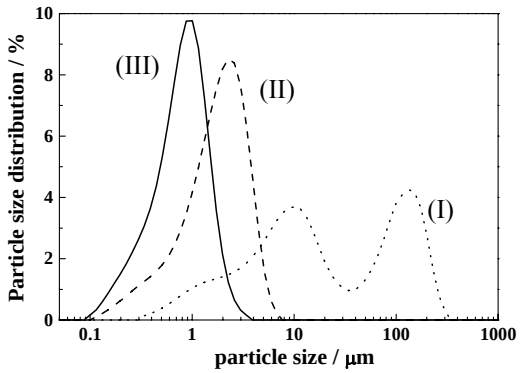

Figure 1: Particle size distribution of LSF powders (I) as-calcined at 1673 K and ground by ball-milling for (II) 10 and (III) 30 h.

3.2 Overpotentals of $La_{0.7}Sr_{0.3}MO_3$ Cathodes

The LSM, LSC, and LSF powders ground by ball milling for 30 h were utilized to elucidate cathode performance. Figure 2 shows the cathodic overpotentials of $La_{0.7}Sr_{0.3}MO_3$ at 773 and 973 K in H_2-O_2 SOFC. The little difference in catholic overpotentials was observed among three electrodes at 973 K. On the other hand, the cathodic overpotential at 773 K largely depended on the kind of perovskite-type oxide; LSF exhibited the lowest cathodic overpotential among three perovskite-type oxides. A similar result was reported for the perovskite-type oxide cathodes fabricated without grinding by ball milling [14].

3.3 Influence of Particle Size of LSF Powder

Figure 3 represents the SEM photographs of interfaces between LSF cathode and SCY electrolyte. The morphologies of LSF (a)-(c) significantly differed from each other. We can see that the LSF (b) and (c) were less porous than LSF (a). This may be due to fine particles and good uniformity in particle size of LSF powder, as shown in Fig. 1. In addition, it seems that LSF (b) and (c) tightly adhered to SCY electrolyte. This implies that there is a fair number of the three phase boundary in LSF (b) and (c), although the gas diffusion in these cathodes may be inhibited due to their dense structures.

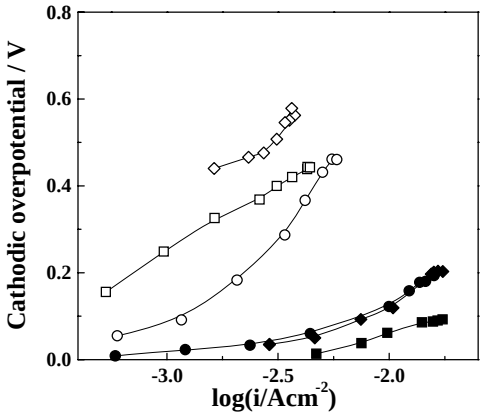

Figure 2 : Cathodic overpotentials of (○, ●) LSF, (□, ■) LSM, and (◊, ♦) LSC at the measurement temperature of (○, □, ◊) 773 and (●, ■, ♦) 973 K.

The cathodic overpotentials of LSF (a)-(c) are depicted in Fig. 4. The overpotential of LSF cathode decreased in the following order: LSF (a) > (b) > (c). The lowest cathodic overpotential was achieved for the LSF (c). Thus, it was found that the cathodic overpotential in H_2-O_2 SOFC using proton conductor is strongly affected by the particle size and distribution of souse powder of cathode material.

The activation energy of electrode reaction can be calculated from the Arrhenius plot of the inverse of the electrode resistance corresponding to the slope of the overpotential against the current density [13]. The activation energies of LSF (a)-(c) are summarized in Table 1, together with that of Pt cathode. The activation energy of Pt cathode was estimated to be 0.90 eV in the temperature range of 773-973 K, being close to the value (0.99 eV) reported by Uchida et al. [13] As can be seen in Table 1, the activation energy of LSF cathode was clearly lower than that of Pt cathode. This result suggests that the rate-determining step of the electrode reaction for LSF cathode is different from that for Pt cathode.

The activation energies of LSF increased in the following order: LSF (a) < (b) < (c). This result suggests that the rate-determining step is changed by the electrode morphology. We have proposed that the elementary step of either water formation (eq. (4)) or water desorption (eq. (5)) is the rate-determining step of cathodic reaction in SOFC using proton conductor [14]. As can be expected from the SEM photographs in Fig. 3, the porosity of LSF cathode decreased in the following order: LSF (a) > (b) > (c), suggesting that the diffusion of water formed was limited in the same order. Therefore, for LSF (c), the desorption/diffusion of water (eq. (5)) is consider to be the rate-determining step. In the case of LSF (a), as the strict limitation of gas diffusion is moderated due to the presence of large-sized pore in electrode, the other elementary step would become the rate-determining step.

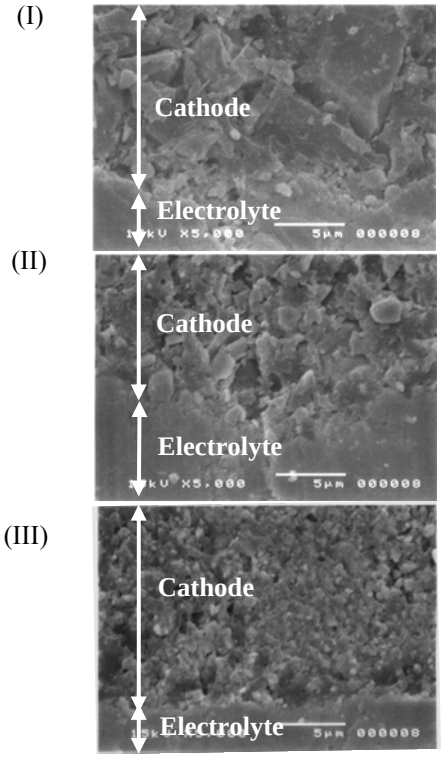

Figure 3: SEM photographs of interface between LSF cathode and SCY electrolyte. (I) LSF (a), (II) LSF (b), and (III) LSF (c).

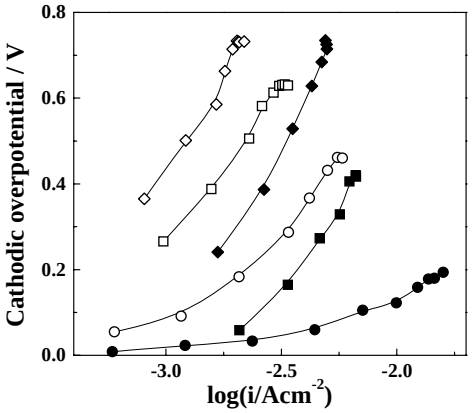

Figure 4: Cathodic overpotentials of (◊, ♦) LSF (a), (□, ■) LSF (b), and (○, ●) LSF (c) at (◊, □, ○) 773 and (♦, ■,●) 973 K.

Cathode	Activation energy / eV
Pt	0.90
LSF (a)	0.36
LSF (b)	0.51
LSF (c)	0.71

Table 1 : Activation energies of LSF (a)-(c) and Pt cathode.

Clean Technology 2008, www.ct-si.org, ISBN 978-1-4200-8502-0

3.4 Fabrication of LSF Cathode by EPD

The electrophoretic deposition (EPD) method was applied to fabricate LSF cathode on electrolyte surface. Figures 5(A) and 5(B) shows the SEM photograph and the overpotentials of LSF cathode fabricated by EPD method (denoted as LSF-EPD). Judging from SEM photograph (Fig. 5(A)), the electrode morphology of LSF-EPD heat-treated at 1173 K was very similar to that of LSF (c) (Fig. 3(III)). As a result, the cathodic overpotential of LSF-EPD was comparable to that of LSF (c). Interestingly, when heat-treatment temperature was reduced to 973 K, the cathodic overpotential of LSF-EPD was remarkably decreased. Therefore, the fabrication of oxide cathode by EPD would be the promising method for realizing IT-SOFC with proton conductor.

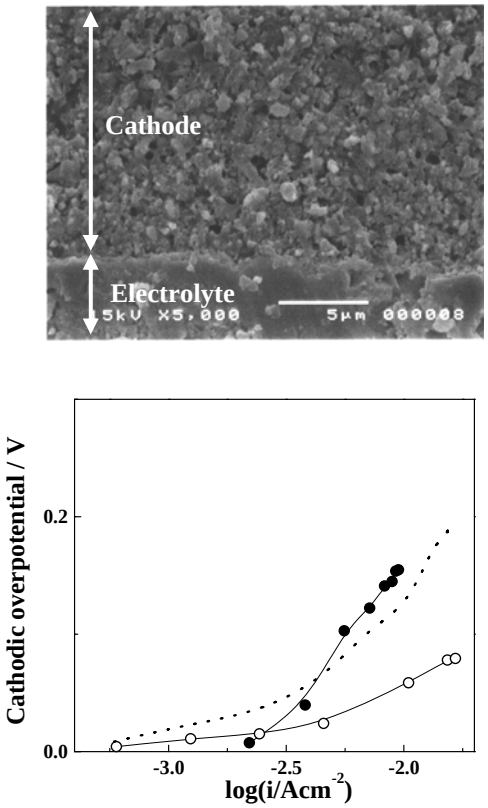

Figure 5 : (A) SEM photograph of LSF-EPD heat-treated at 1173 K. (B) Cathodic overpotentials of LSF-EPD heat-treated at (○) 973 and (●) 1173 K. The dotted line stands for the overpotential of LSF (c). The measurement temperature was 973 K.

4 CONCLUSION

The electrochemical performances of the perovskite-type oxide cathodes with uniform particles were investigated in H_2-O_2 SOFC system using proton conductor. When LSM, LSC, and LSF electrodes with similar particle size distribution were used as a cathode material, the overpotential decreased in the following order: LSC > LSM > LSF. The good performance of LSF cathode was pronounced at lower temperature. The overpotentials of LSF cathode were influenced by the electrode morphologies such as particle size and uniformity; the decrease in the particle size resulted in the decrease in the overpotential. The activation energy of LSF cathode reaction, estimated from the temperature dependence of the overpotential, increased with decreasing the particle size. This result indicates that the rate-determining step of cathode reaction was changed by the electrode morphology. The EPD method was applied to fabricate LSF cathode. It was found that the heat-treatment temperature can be reduced by EPD method, resulting in the decrease in the overpotential of LSF cathode.

REFERENCES

[1] N. Kurita, K. Otsuka, N. Fukatsu, T. Ohnishi, Solid State Ionics 79, 358, 1995.
[2] H. Iwahara, Solid State Ionics 125, 271, 1999.
[3] S. Hamakawa, T. Hibino, H. Iwahara, J. Electrochem. Soc. 141, 1720, 1994.
[4] H. Iwahara, H. Uchida, M. Maeda, J. Power Sources 7, 283, 1982.
[5] H. Iwahara, H. Uchida, S. Tanaka, Solid State Ionics 9/10, 1021, 1983.
[6] H. Iwahara, T. Yajima, T. Hibino, H. Ushida, J. Electrochem. Soc. 140, 1687, 1993.
[7] N. Bonanos, B. Ellis, M. N. Mahmood, Solid State Ionics 44, 305, 1991.
[8] I. Kosacki, H. L. Tuller, Solid State Ionics 80, 223, 1995.
[9] N. Q. Minh, J. Am. Ceram. Soc. 76, 563, 1993.
[10] H. Uchida, S. Arisaka, M. Watanabe, Solid State Ionics 135, 347, 2000.
[11] M. D. Anderson, J. W. Stevenson, S. P. Simner, J. Power Sources 129, 188, 2004.
[12] S. P. S. Badwal, S. P. Jiang, J. Love, J. Nowotny, M. Rekas, E. R. Vance, Ceram. International 27, 419, 2001.
[13] H. Uchida, S. Tanaka, H. Iwahara, Appl. Electrochem. 15, 93, 1985.
[14] H. Yamaura, T. Ikuta, H. Yahiro, G. Okada, Solid State Ionics 176, 269, 2005.
[15] Y. Itagaki, F. Matsubara, M. Asamoto, H. Yamaura, H. Yahiro, Y. Sadaoka, ESC Trans. 7, 1319, 2007.